

Electrolytic Recovery of High Purity Zr from Radioactively Contaminated Zr Alloys in Chloride Salts

Sungjune Sohn¹, Jaeyeong Park^{2,*}, Il Soon Hwang¹

¹ Department of Energy System Engineering, Seoul National University, 1 Gwanak-ro, Gwanak-gu, Seoul 08826, Republic of Korea

² School of Mechanical, Aerospace and Nuclear Engineering, Ulsan National Institute of Science and Technology, 50 UNIST-gil, Ulsu-gun, Ulsan 44919, Republic of Korea

*E-mail: jypark@unist.ac.kr

Received: 9 January 2018 / Accepted: 19 February 2018 / Published: 6 March 2018

It has been believed that high purity Zr metal is hard to be prepared from Zr alloys in LiCl-KCl salts since Zr has various redox reactions in LiCl-KCl including insoluble ZrCl formation and disproportionate reaction between Zr and Zr^{4+} . We examined electrolytic Zr recovery from Zircaloy-4 by controlling anodic potential at five concentrations of $ZrCl_4$ in LiCl-KCl salts. Anode potential of -0.9 V (vs. Ag/AgCl) was applied to prevent the elements except Zr being dissolved from the anode into the electrolyte. Experimental results showed Zr with purity of over 99.9% was recovered and all alloying elements were analyzed below their detection limit in ICP-MS. In addition, at low $ZrCl_4$ concentrations of 0.1 and 0.5 wt.%, the chemical form of the cathode deposits was Zr metal without ZrCl while only ZrCl without Zr metal was recovered at the high $ZrCl_4$ concentration, 2.0 and 4.0 wt.%. At the $ZrCl_4$ concentration of 1.0 wt.%, both Zr metal and ZrCl were recovered. Therefore, preparation of high purity Zr metal from Zr alloys is feasible in LiCl-KCl at low concentration of $ZrCl_4$.

Keywords: Electrolytic recovery, Electrefining, Zr recovery, High Purity Recovery, LiCl-KCl

1. INTRODUCTION

Zirconium based alloys have been utilized in the nuclear fuel due to its low thermal neutron capture cross section and high hardness [1]. Zircaloy hull occupies about 25% of the total mass in spent nuclear fuel (SNF), and the amount of accumulated SNF has been increasing steadily for a few decades [2]. Since irradiated Zircaloy cladding in SNF is classified as an intermediate level waste based on International Atomic Energy Agency (IAEA) radioactive waste criteria due to penetrated

actinides and activation products, it is essential to decontaminate Zircaloy cladding for the radioactive waste management [3-4]. Also, recovery of Zr without other impurities from the Zircaloy hull would be necessary to lower radioactive waste level as well as reduce waste volume.

Several types of research have been conducted for the Zircaloy cladding decontamination both surficial and volumetric methods. Rudisill studied chemical treatment using diluted HF for ZrO_2 layers on the surface of irradiated cladding to remove actinides and fission products [5]. The results showed transuranic elements could penetrate at least 180 μm into the cladding and the decontaminated cladding was still classified as Greater-Than-Class C wastes of the United States. Therefore, the surface decontamination would not be a major priority.

Halogenation methods have been studied for volumetric decontamination of the cladding. Jeon studied chlorination behavior of fresh Zircaloy-4 to separate Zr, and the recovered ZrCl_4 had very high purity [6]. Kroll developed reduction process of ZrCl_4 using Mg reductant as a part of commercialized Zircon sand refining [7-8]. But this process may be hard to be applied to radioactive Zr alloys because MgCl_2 which is the byproduct from the reaction of ZrCl_4 with Mg could be mixed with chlorides of other radioactive elements and it can cause the amount of radioactive waste increasing. Collins conducted two steps iodination processes consisted of the formation and the decomposition of ZrI_4 using non-radioactive Zircaloy [9]. The results showed good Zr recovery performance, but there might be commercialization issues since iodination process requires long reaction time.

Experimental investigations on electrorefining in alkali halides have been conducted for volumetric decontamination of Zircaloy cladding because electrochemical methods are more simple and compact than others. The redox behaviors of Zr in chlorides have been known to be very complicated due to disproportionate reaction [10-14]. There are various soluble states (Zr^{4+} and Zr^{2+}) and insoluble states (Zr metal ZrCl) in molten LiCl-KCl . Hence, current efficiency might be lower, and ZrCl could be co-deposited at cathode in chloride based electrorefining. Sakamura examined chemical forms of Zr deposit according to applied cathode potential [13]. Mostly ZrCl was recovered at the cathode potential of -1.15~-1.04 V (vs. Ag/AgCl). Zr metal was produced with a little ZrCl when the cathode potential was controlled between -1.42 and -1.35 V (vs. Ag/AgCl). Lee conducted electrorefining of an unirradiated Zircaloy-4 piece in LiCl-KCl salts with 4 wt.% ZrCl_4 by applying three constant cathode potentials, but complete suppression for ZrCl deposition was not achieved [14].

The redox behavior of Zr in fluorides is simple as Zr(IV) is directly reduced to Zr metal [15-17]. Park conducted electrorefining using nuclear grade Zirlo scrap under four applied current conditions at 700°C in LiF-KF-ZrF_4 salts to recover coarse Zr deposit [16]. The results showed all recovered Zr contained impurities less than 700 ppm. Fujita introduced LiF (10 mol%) added LiCl-KCl-ZrCl_4 system for irradiated BWR channel box electrorefining by applying anode current density of 0.1A/cm^2 at 650°C [17]. After two steps electrorefining, the decontamination factor of Co-60 was produced to 4×10^4 . Lee investigated Zirlo electrorefining and showed the morphological enhancement of cathode deposits in fluoride added chloride salts to compare with the results from all-chloride salts based electrorefining [18]. Although fluorides based electrorefining have some advantages in terms of the process efficiency and the recovery of cathodic deposits, there are some concerns on scale-up. Operating temperatures are higher than that of chlorides based electrorefining. Also, corrosion issues for the structural materials of electrorefining should be considered.

In this study, therefore, chlorides based lab-scale Zircaloy-4 electrorefining experiments were conducted to recover metallic Zr with high purity under the suppression of the ZrCl deposition. Based on the previous study, the electrorefining experiments were performed by controlling anode potential at five different salt compositions as ZrCl₄ concentrations changed [19]. After electrorefining, chemical analyses on cathode deposits and used salts were carried out to investigate the purity and composition of cathodic products by X-ray Diffraction (XRD) and inductively coupled plasma-mass spectrometry (ICP-MS).

2. EXPERIMENTAL

2.1. Reagent preparation

Anhydrous LiCl-KCl eutectic beads and ZrCl₄ powders with purity of 99.99% were supplied from the Sigma Aldrich and used for the molten salt electrolyte. Chloride solution of LiCl-KCl-ZrCl₄ (10 wt.%) was firstly produced and it is diluted down to the concentrations for each electrorefining experiments (0.1, 0.5, 1.0, 2.0 and 4.0 wt.% of ZrCl₄ in LiCl-KCl eutectic). ZrCl₄ sublimates at 331°C which is lower than the melting point of LiCl-KCl eutectic (353°C) but the loss of ZrCl₄ due to its sublimation can be prevented once it is dissolved in LiCl-KCl [11]. Therefore, to melt LiCl-KCl and dissolve ZrCl₄ into the melts rapidly, the quartz cell containing LiCl-KCl beads and 10 wt.% ZrCl₄ powders was placed into the furnace heated to 600°C. A narrow quartz cell with an inner diameter of 11 mm was used, and LiCl-KCl beads were stacked up on the ZrCl₄ powders placed on the bottom of the cell in order to catch the sublimated ZrCl₄. A cold trap at the top of the quartz cell was also set up to identify the sublimation of ZrCl₄, but ZrCl₄ powders were not observed [19].

2.2. Experimental setup

All electrochemical experiments were carried out in a glove box filled with argon gas with 99.999% purity. The concentrations of oxygen and moisture inside glove box were maintained below 0.1 ppm during the experiments. The schematic diagram of apparatus for high temperature experiments and the optical photograph of the electrorefining cell configuration are prepared as shown in Figure 1. The electrochemical cell was placed inside furnace made of type 304 SS installed at the bottom of the glove box. A quartz cell with an inner diameter of 27 mm, an outer diameter of 30 mm and a height of 380 mm was used for the LiCl-KCl-ZrCl₄ container. The cell temperature was directly measured during the electrorefining using a K-type thermocouple. The temperature of molten salts was maintained to 500 °C within ± 1 °C using proportional-integral-derivative (PID) heater controller. Potential was applied and controlled by using VersaStat3 potentiostat with VersaStudio software.

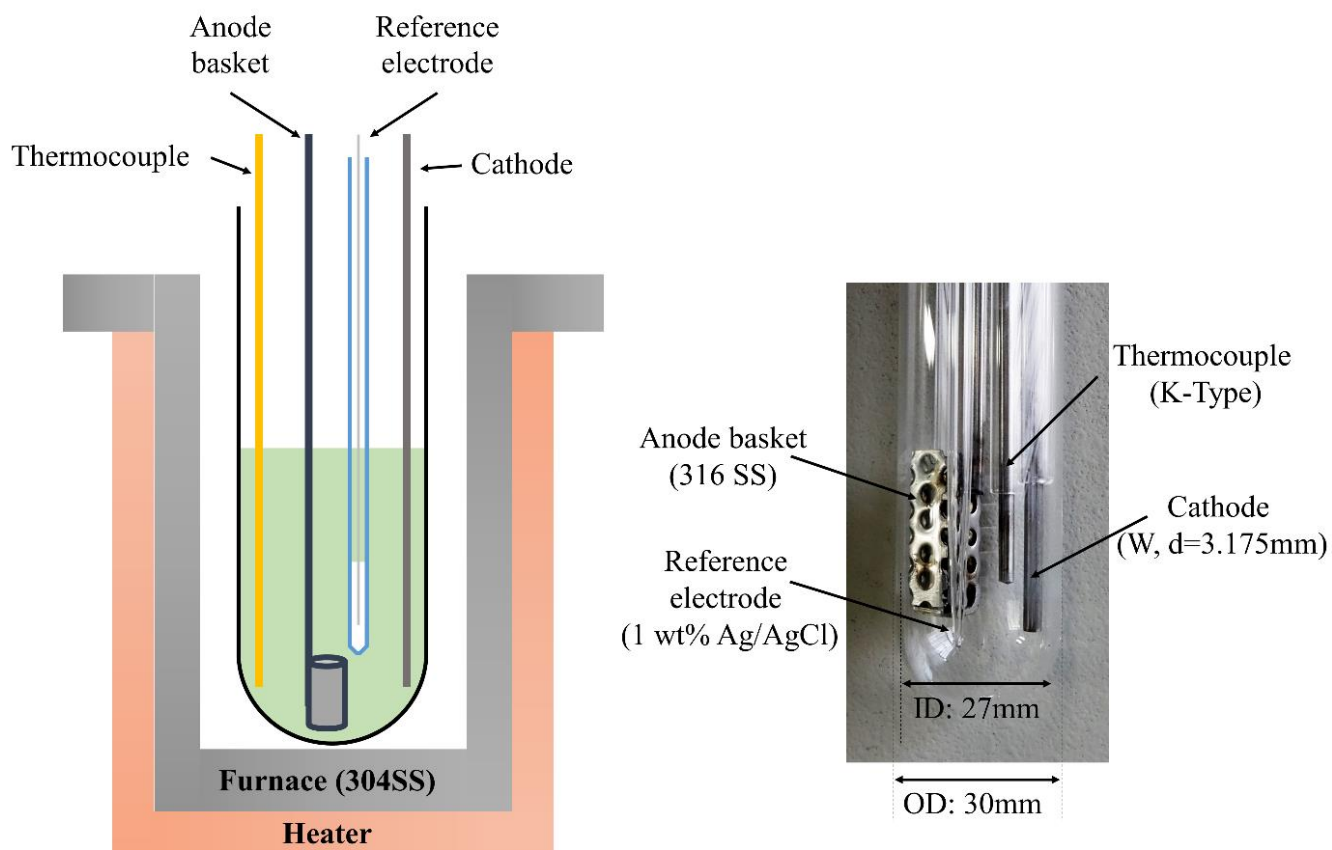


Figure 1. (Left) Schematic diagram of the Zircaloy-4 electrorefining cell and (right) optical photograph of electrorefining cell configuration

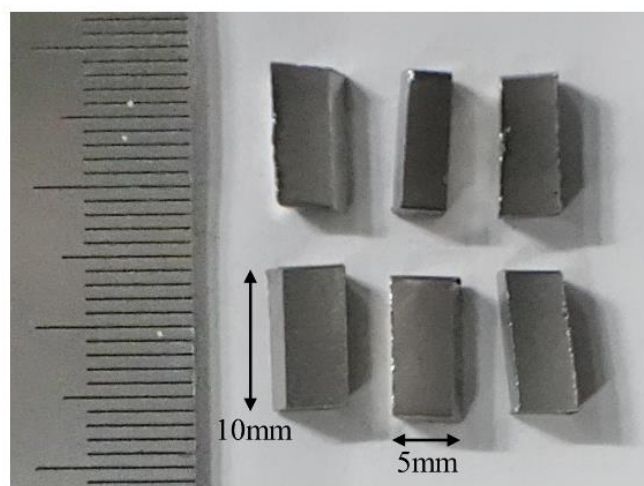


Figure 2. Unirradiated Zircaloy-4 cuts utilized for the electrorefining experiments

For lab-scale electrorefining experiments, three electrodes system were applied as represented in Figure 1. Ag/AgCl reference electrode made of a thin Pyrex cell, silver wire (Sigma Aldrich, 99.9% purity, 1mm diameter) and LiCl-KCl-AgCl (1 wt.%) were utilized. Tungsten rod (Alfa Aesar, 99.95% purity, 3.175 mm diameter) was used for the cathode. A basket made of 316 stainless steel with each side of 10 mm and height 30 mm was designed as an anode basket to contain the Zircaloy-4 specimens. Six cuts of the Zircaloy-4 prepared from a Zircaloy-4 tube were loaded into the anode basket as shown in Figure.2. The composition of the Zircaloy-4 specimen was analyzed by ICP-MS as represented in Table 1. The Zircaloy-4 was mainly composed of Zr of 98.6 wt.% and small amounts of Sn, Cr, and Fe as alloying elements. Co was also analyzed since it is one of the impurity elements of Zircaloy-4 and Co-60 is the most important isotope, which should be considered in terms of irradiated SNF Zircaloy-4 cladding decontamination. [3].

Table 1. Composition of unirradiated Zircaloy-4 specimen utilized for the electrorefining experiments analyzed by ICP-MS

Element	Composition (wt.%)
Zr	98.6
Sn	1.12
Cr	0.083
Fe	0.161
Co	0.0016
Etc.	0.0344
Total	100

2.3. Electrorefining of Zircaloy-4

According to the author's previous study on ZrCl_4 cyclic voltammetry, the redox behavior of Zr in LiCl-KCl including insoluble ZrCl and Zr metal formation is greatly complicated, and each redox reaction rate can be significantly influenced by the ZrCl_4 concentration [19]. In the cyclic voltammograms, the oxidation peak height of ZrCl diminishes as ZrCl_4 concentration decreases. Therefore, it is expected that cathodic deposits would be Zr metal under the electrorefining at a low concentration of ZrCl_4 whereas ZrCl would be deposited at high concentration of ZrCl_4 . From this expectation, electrorefining experiments were carried out in the electrolyte of the five different ZrCl_4 concentrations (0.1, 0.5, 1.0, 2.0 and 4.0 wt.% of ZrCl_4 in LiCl-KCl eutectic) to investigate the effects of initial salt concentrations on the chemical forms of Zr deposits.

In all five electrorefining experiments, anode potential was maintained as a constant voltage to suppress dissolution of all alloying elements (Sn, Cr, and Fe) and Co. The apparent standard potentials of the Sn^{2+}/Sn , Cr^{2+}/Cr , Fe^{2+}/Fe , Co^{2+}/Co , and $\text{Zr}^{4+}/\text{ZrCl}$ in LiCl-KCl at 500°C that were measured in the equivalent electrochemical system of this study are represented in Table 2 [19]. Since all of the alloying elements (Sn, Cr, Fe) and Co are nobler than $\text{Zr}^{4+}/\text{ZrCl}$ reaction, these elements would be deposited on the cathode and the purity of Zr recovered on the cathode would decrease if the elements are dissolved from the anode basket into the molten salts. Cr is the noblest elements among these

elements with the apparent standard potential of -0.898 V (vs. Ag/AgCl). Therefore, anode potential is maintained at -0.9 V (vs. Ag/AgCl) for all electrorefining experiments.

Table 2. Apparent reduction potentials of the alloying elements (Sn, Cr and Fe) of Zircaloy-4 and Co in LiCl-KCl at 500°C.

Reaction	Apparent reduction potential [19] (V vs. Ag/AgCl)
$\text{Zr}^{4+}/\text{ZrCl}$	-1.503
Sn^{2+}/Sn	-0.510
Cr^{2+}/Cr	-0.898
Fe^{2+}/Fe	-0.620
Co^{2+}/Co	-0.426

After electrorefining, chemical forms and compositions of the deposits and salts were analyzed by XRD and ICP-MS respectively. The cathode deposits were scrapped, and sealed in a sample bottle to prevent oxidation of the products before XRD and ICP-MS analysis. The XRD was also applied to the LiCl-KCl and LiCl-KCl-ZrCl₄ (10 wt.%) to compare with the XRD results after electrorefining as represented in Figure 3.

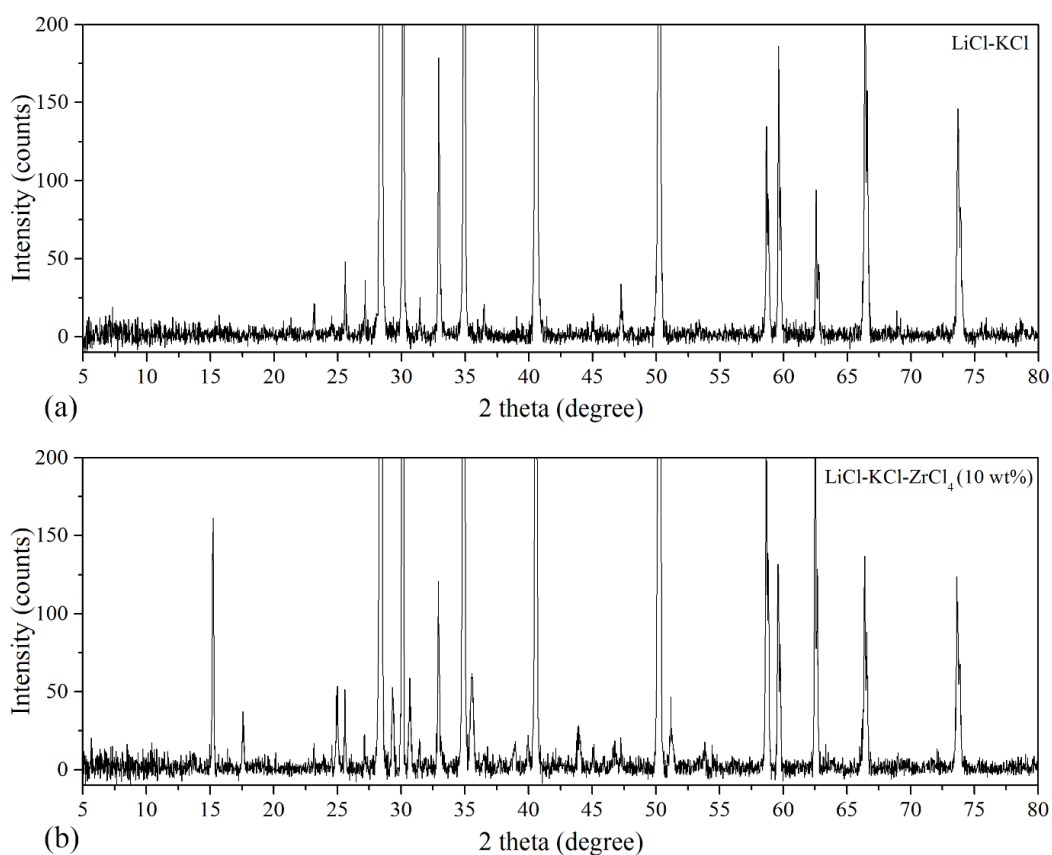


Figure 3. XRD results for (a) LiCl-KCl and (b) LiCl-KCl-ZrCl₄ (10 wt.%)

3. RESULTS

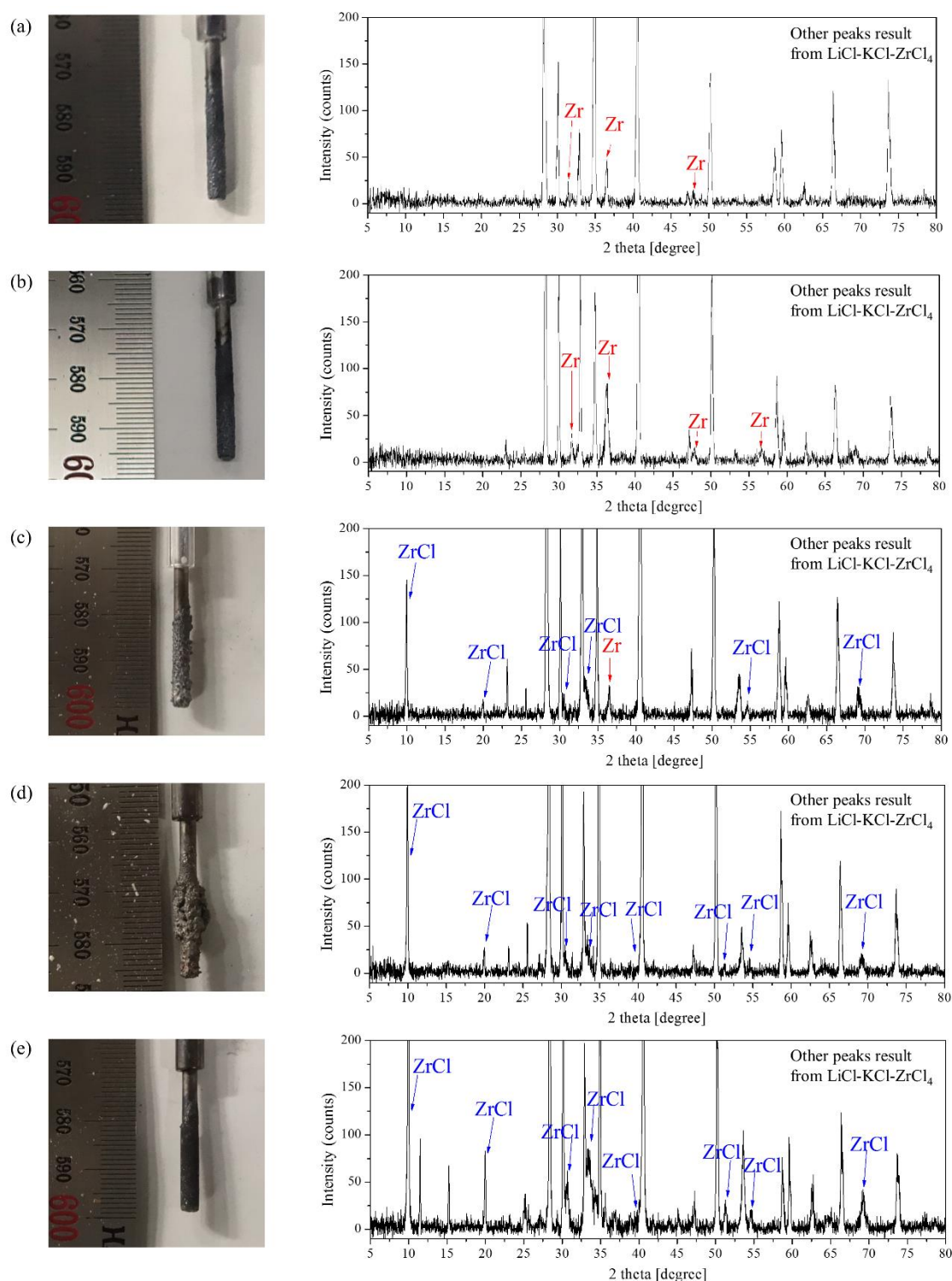


Figure 4. (Left) Optical photographs and (right) analysis results via XRD of the cathode deposits after the electrorefining experiments at the ZrCl_4 concentration of (a) 0.1, (b) 0.5, (c) 1.0, (d) 2.0 and (e) 4.0 wt. %

In all electrorefining experiments, the powdery cathode deposits were collected. The compositions of the cathode deposits are summarized in Table 3. Alloying elements (Sn, Cr, Fe) and Co were not found in the ICP-MS results beyond the detection limit. When considering the detection

limit of each element and unconsidered impurities, the purity of Zr in the cathode deposits would be over 99.9% if the trapped salts in the cathode deposits were removed.

Optical photographs of the cathodes after electrorefining and XRD results on the deposits are represented in Figure 4. In the XRD results of Figure 4, unmarked peaks are matched to the peak of LiCl-KCl or LiCl-KCl-ZrCl₄ (10 wt.%). In the cases that the initial ZrCl₄ concentrations in the electrolyte are 0.1 and 0.5 wt.%, Zr metal was recovered without ZrCl. As the increase of the ZrCl₄ concentration, ZrCl becomes dominant in the deposits. At the ZrCl₄ concentration of 1.0 wt.%, both Zr metal and ZrCl were recovered. At the higher concentrations of ZrCl₄, 2.0 and 4.0 wt.%, only ZrCl without Zr metal was deposited on the cathode.

Table 3. Composition and chemical form of the cathodic deposits after electrorefining experiments

		This study					Lee [14]	
ZrCl ₄ concentration (wt.%)		0.1	0.5	1.0	2.0	4.0	4.0	4.0
Operating condition		Anode potential maintained at -0.9 V					Cathode potential maintained at -1.15 V	Cathode potential maintained at -1.55V
Composition of cathode deposits (wt.%)	Zr	Over 99.9	Over 99.9	Over 99.9	Over 99.9	Over 99.9	99.44	98.95
	Sn	N/D	N/D	N/D	N/D	N/D	0.56	0.87
	Cr	N/D	N/D	N/D	N/D	N/D	N/D	0.14
	Fe	N/D	N/D	N/D	N/D	N/D	N/D	0.04
	Co	N/D	N/D	N/D	N/D	N/D	Not analyzed	
Chemical form of zirconium deposits		Zr	Zr	Zr and ZrCl	ZrCl	ZrCl	ZrCl and Zr	

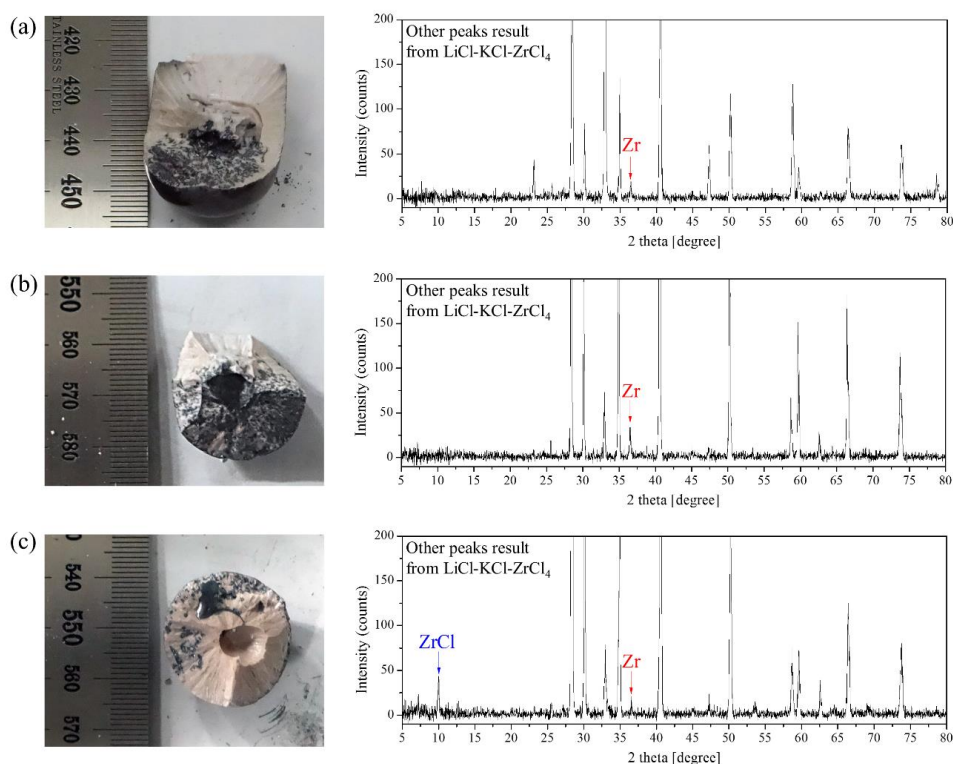


Figure 5. (Left) Optical photographs and (right) analysis results via XRD of the used salt ingots after electrorefining experiments at the ZrCl₄ concentration of (a) 0.1, (b) 0.5, (c) 1.0 wt.%

Figure 5 and Figure 6 represents the optical photographs of the used salt ingots in a cross sectional view. In the case of 0.1, 0.5 and 1.0 wt.%, there were black powdery precipitates in the bottom part of the ingots but they are not observed at the concentration of 2.0 and 4.0 wt.%. The salt ingots containing black powders were cut into several pieces, and the bottom parts with black powders were collected. The collected bottom salts were analyzed by XRD to identify chemical forms of the black powders as represented in Figure 6. XRD results indicate that black powders were Zr metal in the electrorefining using 0.1 and 0.5 wt.% of ZrCl_4 while the black powders were the mixture of Zr metal and ZrCl for the molten salts with 1.0 wt.% ZrCl_4 . After electrorefining under the ZrCl_4 concentrations of 2.0 and 4.0 wt.%, black powdery precipitates were not observed at the bottom of the salt ingots as represented in Figure 6. Colors of the molten salt ingots are shown to become darker from light brown to dark brown as the ZrCl_4 concentration increases.



Figure 6. Optical photographs of the used salt ingots after electrorefining in (left) LiCl-KCl-ZrCl_4 (2.0 wt.%) and (right) LiCl-KCl-ZrCl_4 (4.0 wt.%)

4. DISCUSSION

4.1. Composition of cathodic deposits

Since the anode potential was controlled as -0.9 V (vs. Ag/AgCl) which is a slightly negative value of the apparent reduction potential of Cr in LiCl-KCl at $500\text{ }^\circ\text{C}$, only Zr was dissolved as Zr^{4+} ion from Zircaloy-4 cuts into the electrolyte and the other elements were not oxidized into the ions. The anode potential control method leads the results that very high purity of Zr was deposited on the cathode. Lee et al. conducted electrorefining experiments with Zircaloy-4 specimen in LiCl-KCl at the ZrCl_4 concentration of 4 wt.% by controlling the cathode potential [14]. The cathode potential was controlled to investigate the chemical form of the cathode. The cathode deposits obtained by the cathode potential control electrorefining contained Sn and other elements as represented in Table 3.

These results would imply that electrorefining would be an effective decontamination process for irradiated Zircaloy-4 cladding if an anode potential is maintained constantly during the process. These methodological approaches could be applied to other Zr alloys which have been utilized in the nuclear industry such as Zirlo and Zr-2.5Nb because alloying elements of those including Nb are nobler than Zr [20-22]. If electrorefining for the Zr alloys is operated in a galvanostatic condition, the termination time of the electrorefining should be determined by monitoring the point that anode

potential gets more positive value than the apparent standard potential of the most oxidative element except Zr.

Sn was not observed at both the cathodic deposits and the bottom of the used salt ingots for all electrorefining conditions. That could be attributed to relatively short operation time, but there is a concern related to the melting of Sn. The melting point of Sn is about 232°C which is much lower than the operating temperature. According to the binary phase diagram of Zr-Sn, Sn forms a solid solution with Zr at the initial stage of electrorefining because the composition of Sn in Zircaloy-4 is approximately 1 wt.% so Sn might not melt out from Zircaloy-4 cuts [23, 24]. If the electrorefining is operated until most of Zr in the Zircaloy-4 specimen is depleted, the local concentration of Sn in the Zircaloy-4 specimen would increase sharply. As the concentration of Zr decreases, Sn-rich intermetallic compound would finally be decomposed, and Sn would exist as a liquid phase in the anode basket. As a result, Sn could melt out from Zircaloy-4 cuts at the end stage of the electrorefining. If Sn melts out from the anode, Sn might not be deposited but be trapped with LiCl-KCl and inside the cathodic deposits. That would result in decreasing the recovered Zr purity. Therefore, operating conditions to minimize Sn melting should be developed to recover Zr without Sn.

4.2. Powdery cathode deposits and precipitate on the bottom of the used salt ingots

Morphological characteristics of Zr in both the cathodic deposits and the bottom of the molten salts are shown to be a powdery shape. Powdery products would have some concerns in a post-process after electrorefining for the recovered metal to be utilized because it could be easy to be oxidized. If oxygen content exceeds 0.7% in zirconium compounds, Zr would become unworkable, and reactor-grade Zr requires oxygen content lower than 1,000 ppm [25]. Therefore, melting and casting processes should be applied to powdery Zr to minimize oxidation as soon as possible after electrorefining of Zr alloys. Arc melting process was proven practically for Zr powder to be converted into Zr sponge which can satisfy ASTM B349 specifications for nuclear-grade [16]. If the electrorefining is conducted using irradiated Zircaloy-4, recovered Zr contains Zr-93 which cause radioactivity in the Zr lumps is approximately 300 times larger than its clearance level and it would be difficult to be utilized under radiation-free environment [3]. However, recovered Zr produced by arc melting would be utilized to materials for a part of radioactive waste disposal container as well as for fabricating metallic fuels for fast reactors and inert matrix for transmutation targets fabrication.

Black powders were observed in the bottom of the molten salts after electrorefining in ZrCl_4 of 0.1, 0.5 and 1.0 wt.% in the molten salts and the chemical forms were equivalent to cathodic deposits. From the results, it could be deduced from the results that disproportionate reactions forming ZrCl would be greatly slow. ZrCl could be produced by a disproportionate reaction in chloride salts such as KCl-NaCl-CsCl as follow [25]:



The Gibbs free energy of reaction (1) calculated by HSC chemistry 5 is -36 kJ at 500°C, so it is a spontaneous reaction. If the reaction rate of the reaction (1) were fast enough to produce ZrCl, ZrCl would be found at the bottom of both 0.1, and 0.5 wt.% ZrCl_4 salt ingots but ZrCl was not detected in

this condition. That could indicate that decrease of Zr recovery efficiency resulting from the ZrCl formation would be negligible. Therefore, the powdery precipitates at the bottom of the salts would be recycled if electrefining of Zircaloy-4 is operated at the condition that Zr metal is deposited without ZrCl.

4.3. Chemical form of the Zr deposits according to ZrCl₄ concentration

As the concentration of ZrCl₄ which is used as an initiator for electrefining increases, more amount of ZrCl would be recovered with Zr metal. As a result, low concentration of ZrCl₄ would be preferred to recover Zr metal without ZrCl. This phenomenon could be explained by the reduction mechanism of Zr as follow [3]:



If the forward reaction rate of reaction (2) is faster than that of reaction (3), ZrCl would be maintained in the cathodic deposits. On the other hand, if the forward reaction rate of reaction (2) is slower than that of reaction (3), all of ZrCl would be converted into Zr, and only Zr metal was recovered on the cathode.

The electrochemical reaction rates are greatly depending on applied current density or applied potential and concentrations of the reactants and products. The mole production rate of ZrCl in the reaction (2), \dot{m}_{ZrCl} could be determined by equation (4) [26].

$$\begin{aligned} \dot{m}_{\text{ZrCl}} &= -\frac{i_{\text{ZrCl}}}{n_{\text{ZrCl}}F} \\ &= -k_{0,\text{ZrCl}}[-C_{\text{Zr}^{4+}}(0,t)\exp(-\alpha_{\text{ZrCl}}\frac{n_{\text{ZrCl}}F}{RT}(E-E_{\text{ZrCl}}^{0'})) + \exp((1-\alpha_{\text{ZrCl}})\frac{n_{\text{ZrCl}}F}{RT}(E-E_{\text{ZrCl}}^{0'}))] \end{aligned} \quad (4)$$

where i_{ZrCl} is the current density resulting from the reaction of ZrCl formation, n_{ZrCl} is the number of electrons participating in the reaction of ZrCl formation, F is the Faraday constant, $k_{0,\text{ZrCl}}$ is the rate constant for the reaction of ZrCl formation, $C_{\text{Zr}^{4+}}(0,t)$ is the surface concentration of Zr^{4+} , α_{ZrCl} is the charge transfer coefficient for the ZrCl formation, E is the electrode potential, $E_{\text{ZrCl}}^{0'}$ is the formal potential of the ZrCl formation, R is the universal constant and T is the temperature. The mole production rate of Zr in the reaction (3), \dot{m}_{Zr} would be determined by equation (5) [26].

$$\begin{aligned} \dot{m}_{\text{Zr}} &= -\frac{i_{\text{Zr}}}{n_{\text{Zr}}F} \\ &= -k_{0,\text{Zr}}[-\exp(-\alpha_{\text{Zr}}\frac{n_{\text{Zr}}F}{RT}(E-E_{\text{Zr}}^{0'})) + \exp((1-\alpha_{\text{Zr}})\frac{n_{\text{Zr}}F}{RT}(E-E_{\text{Zr}}^{0'}))] \end{aligned} \quad (5)$$

where i_{Zr} is the current density resulting from the reaction of Zr formation, n_{Zr} is the number of electrons participating in the Zr formation, $k_{0,\text{Zr}}$ is the rate constant for the reaction of Zr formation, α_{Zr} is the charge transfer coefficient for the Zr formation and $E_{\text{Zr}}^{0'}$ is the formal potential of the Zr metal formation.

Comparing with equation (4) and equation (5) the current density for ZrCl formation from Zr^{4+} is proportionate to the surface concentration of Zr^{4+} . However, the current density for Zr metal

formation from ZrCl does not depend on the concentration of Zr^{4+} . It indicates that if the initial concentration of ZrCl_4 increases, the reaction rate of the ZrCl formation from Zr^{4+} would increase at the given electrode potential, E , whereas that of Zr metal formation from ZrCl does not change. Therefore, more negative potential should be applied to the cathode to reduce ZrCl into Zr metal completely at a high ZrCl_4 concentration compared with a low ZrCl_4 concentration.

In the electrorefining experiments that Lee conducted at 4 wt.% ZrCl_4 , ZrCl was deposited with Zr metal even highly negative potential was applied to the cathode as represented in Table 3 [14]. The results of electrorefining conducted by Lee et al. accord with the results of this study identifying that ZrCl is likely to be deposited during electrorefining at high concentration of ZrCl_4 . If more highly negative potential had been applied on the cathode in the experiment of Lee et al, all of ZrCl would be reduced into Zr metal but the cathode deposits would contain more Sn, Fe, and Cr. From these results, it would be suggested that electrorefining of Zircaloy-4 should be carried out at low concentration of ZrCl_4 , less than 1 wt% to recover high purity Zr metal without ZrCl .

5. CONCLUSIONS

To better understand Zr alloys electrorefining in LiCl-KCl salts lab-scale electrorefining experiments were conducted using unirradiated Zircaloy-4 specimens at five different concentrations of ZrCl_4 (0.1, 0.5, 1.0, 2.0, 4.0 wt.%) by maintaining anode potential as -0.9 V (vs. Ag/AgCl) at 500 °C. Zr metal was recovered on the cathode without ZrCl at a low concentration of ZrCl_4 (0.1 and 0.5 wt.%), and ZrCl was recovered on cathode at high concentration of ZrCl_4 (2.0 and 4.0 wt.%) revealed by XRD analysis. At the ZrCl_4 concentration of 1 wt.%, both Zr metal and ZrCl were deposited on the cathode. For all cases of electrorefining, highly pure Zr with a purity of over 99.9% was found in the cathode deposits without other alloying elements revealed by ICP-MS analysis. Therefore, chlorides based electrorefining for Zr alloys is identified to be possible to recover high purity Zr metal without ZrCl deposition. Furthermore, ZrCl_4 concentration of 0.5 wt.% would be recommendable for the initiator of Zircaloy-4 electrorefining to get high throughput in our experimental conditions.

ACKNOWLEDGEMENTS

This work was supported by the New Faculty Research Fund (Project Number_1.170100.01) of UNIST (Ulsan National Institute of Science & Technology).

References

1. G.P. Sabol and E. Bradley, Zirconium in the nuclear industry: eleventh international symposium, ASTM International, (1996) West Conshohocken, PA, USA.
2. E.D. Collins, G.D. DelCul, B.B. Spencer, R.R. Brunson, J.A. Johnson, D.S. Terekhov and N.V. Emmanuelg, *Procedia Chemistry*, 7 (2012) 72.
3. J. Park, S. Choi, S. Sohn, K.R. Kim and I.S. Hwang, *Nuclear Engineering and Design*, 275 (2014) 44.

4. R. Restani, E. Aerne, G. Bart, H. Linder, A. Muller and F. Petrik, Characterisation of PWR Cladding Hulls from Commercial Reprocessing, NAGRA, (1992) Wettingen, Switzerland.
5. T.S. Rudisill, *Journal of Nuclear Materials*, 385 (2009) 193.
6. M.K. Jeon, K.H. Kang, G.I. Park and Y.S. Lee, *Journal of Radioanalytical Nuclear Chemistry*, 292 (2012) 513.
7. W. Kroll, A. Schlechten and L. Yerkes, *Transactions of The Electrochemical Society*, 89 (1946) 263.
8. W. Kroll, A. Schlechten, W. Carmody, L. Yerkes, H. Holmes and H. Gilbert, *Transactions of The Electrochemical Society*, 92 (1947) 99.
9. E.D. Collins, G.D. Del Cul, D.S. Terekhov and N.V. Emmanuel, Recycle of Zirconium from Used Nuclear Fuel Cladding: A Major Element of Waste Reduction, WM2011 Conference, Phoenix, AZ, U.S.A. 2011.
10. R. Baboian, D. Hill and R. Bailey, *Journal of The Electrochemical Society*, 112 (1965) 1221.
11. S. Ghosh, S. Vandarkuzhali, P. Venkatesh, G. Seenivasan, T. Subramanian, B.P. Reddy and K. Nagarajan, *Journal of Electroanalytical Chemistry*, 627 (2009) 15.
12. J. Park, S. Choi, S. Sohn, K.R. Kim and I.S. Hwang, *Journal of The Electrochemical Society*, 161 (2014) H97.
13. Y. Sakamura, *Journal of The Electrochemical Society*, 151 (2004) C187.
14. C.H. Lee, K.H. Kang, M.K. Jeon, C.M. Heo and Y.L. Lee, *Journal of The Electrochemical Society*, 159 (2012) D463.
15. H. Groult, A. Barhoun, H. El Ghallali, S. Borensztjan and F. Lantelme, *Journal of The Electrochemical Society*, 155 (2008) E19.
16. K.T. Park, T.H. Lee, N.C. Jo, H.H. Nersisyan, B.S. Chun, H.H. Lee and J.H. Lee, *Journal of Nuclear Materials*, 436 (2013) 130.
17. R. Fujita, H. Nakamura, Y. Haruguchi, R. Takahashi, M. Sato, T. Shibano, Y. Ito, T. Goto, T. Terai and S. Ogawa, Development of zirconium recovery process for zircaloy claddings and channel boxes from boiling water reactors by electrorefining in molten salts, ICAPP '05, Seoul, Korea, 2005.
18. C.H. Lee, D.Y. Kang, M.K. Jeon, K.H. Kang, S. Paek, D. Ahn and K. Park, *International Journal of Electrochemical Science*, 11 (2016) 566.
19. J. Park, S. Choi, S. Sohn and I.S. Hwang, *Journal of The Electrochemical Society*, 164 (12) (2017) D744.
20. J. Park, T. Na, T. Lee, J. Lee, B. Lee and J. Kim, *Journal of Nuclear Science and Technology*, 52 (2015) 748.
21. ASTM B353-12, Standard Specification for Wrought Zirconium and Zirconium Alloy Seamless and Welded Tubes for Nuclear Service (Except Nuclear Fuel Cladding), ASTM International, (2017) West Conshohocken, PA, U.S.A.
22. M. Iizuka, T. Inoue, O. Shirai, T. Iwai and Y. Arai, *Journal of Nuclear Materials*, 297 (2001) 43.
23. R.J. Pérez, C. Toffolon-Masclet, J.M. Joubert and B. Sundman, *Computer Coupling of Phase Diagrams and Thermochemistry*, 32 (2008) 593.
24. H. Okamoto, *Journal of phase equilibria and diffusion*, 31 (2010) 411.
25. G.J. Kipouros and S.N. Flengas, *Journal of The Electrochemical Society*, 132 (1985) 1087.
26. J. Park, Electrorefining of irradiated spent nuclear fuel Zircaloy-4 cladding in LiCl-KCl molten salts, Ph.D. dissertation, Seoul National University, (2014) Seoul, Republic of Korea.